JIPK. Volume 16 No 1 April 2024
Sinta 1 (Decree No: 158/E/KPT/2021)
e-ISSN:2528-0759; p-ISSN:2085-5842
Available online at https://e-journal.unair.ac.id/JIPK

JIPK
(JURNAL ILMIAH PERIKANAN DAN KELAUTAN)
Scientific Journal of Fisheries and Marine

Research Article

Spatial and Temporal Variability of Mixed Layer Depth (MLD) in Eastern Indian Ocean (EIO): 1998-2020

Amir Yarkhasy Yuliardi[1]* and Randi Firdaus[2]

[1]Department of Marine Science, Faculty of Fisheries and Marine, Universitas PGRI Ronggolawe, Tuban, East Java, 62381. Indonesia
[2]Center for Marine Meteorology, Agency for Meteorology Climatology and Geophysics (BMKG), Jakarta, 10610. Indonesia

OPEN ACCESS

ARTICLE INFO

Received: March 09, 2023
Accepted: November 29, 2023
Published: December 03, 2023
Available online: Jan 27, 2024

*) Corresponding author:
E-mail: amiryarkhasy@gmail.com

Keywords:
Mixed Layer Depth
Eastern Indian Ocean
Spatial Variability
Temporal Variability
Sea Surface Temperature

Abstract

Mixed Layer Depth (MLD) plays an important role in various aspects of oceanography. MLD has a characteristic parameter value that is uniform with depth. MLD has an important role for local, regional, and global phenomena. Indonesia, which is surrounded by the East Indian Ocean, will be directly influenced by the dynamics of MLD. This study aimed to analyze seasonal variability and MLD between years. Mixed layer depth data from the ARMOR3D Dataset Copernicus-Marine Environment Monitoring Service was used for MLD analysis with a threshold of 0.2°C for temperature. Wavelet analysis showed that MLD variability in the eastern Indian Ocean spans from intra-seasonal to interannual scales. Time series analysis showed a complex relationship between MLD and SST in the annual and interannual periods which indicates a different process. The MLD monthly climatology at point 90E, 0 showed the depth of mixed layers is deeper during the east monsoon (JJA-SON) ranging from 50-65 m compared to the west monsoon (DJF-MAM) which has a range of 20-40 m. Spatially the MLD in the south of the equator is deeper than in the north. Interannually, MLD is heavily influenced by the Indian Ocean Dipole. MLD depth is deeper in nIOD with a maximum depth in the range of 100 m compared to pIOD. MLD with maximum depth in the strong nIOD phase is around the equator and the pIOD phase is south of the equator. The study also showed that inter-annual variability in regions around the mainland showed a stronger response.

Cite this as: Yuliardi, A.Y., & Firdaus, R. (2024). Spatial and Temporal Variability of Mixed Layer Depth (MLD) in Eastern Indian Ocean (EIO): 1998-2020. *Jurnal Ilmiah Perikanan dan Kelautan*, 16(1):92-105. http://doi.org/10.20473/jipk.v16i1.44026

1. Introduction

Research on the top layer Indian Ocean and the depth of the mixed layer (hereinafter referred to as MLD) in general has been widely carried out. MLD is defined as a layer that has oceanographic parameter values with homogenous values for depth. Homogeneous layers are due to vertical vortex mixing, especially wind pressure on the top layer. In contrast, other convective mixing is usually driven by heat loss to the atmosphere and the flow of fresh water from the atmosphere (Ushijima and Yoshikawa, 2019). The influx of fresh water from rain and surface heating increases surface buoyancy, forming relatively warm and fresh thin MLDs (Yoshikawa, 2015). MLD exhibits spatiotemporal variability and varies at different time scales (Abdulla *et al*., 2016, 2018). MLD has the role of being a source of water movement in the ocean through it because the transfer of mass, momentum and energy occurs in this layer (Yu *et al*., 2020). Mixed layer depth determines the heat content of the ocean (Rugg *et al*., 2016). The heat contained in the MLD has an important role in ocean-atmosphere interactions such as the formation of convection or cyclones (Besa *et al*., 2018). Early research on MLD conducted by Rao *et al*. (1989) through limited observations focused on seasonal cycles. based on the research of Rao and Sivakumar (2000) through climatological observations of global sea temperature, it is characterized by near-surface seasonal variability of the Indian Ocean in isothermal layers. Analysis of heat budget appears as a variable that includes relative heat flux, horizontal advection and vertical entrainment that causes cooling. Meanwhile, seasonal cycles that affect the thickness of the MLD correlate with the monsoonal ecosystem circulation in the Indian Ocean (Xue *et al*., 2021). Mixed layer is critical for phytoplankton development (Schofield *et al*., 2018; Smith Jr and Jones, 2015) and primary productivity through transfer of nutrients related to marine biology (Itoh *et al*., 2015). Mixed layer depth information is useful for fishermen to determine hook depth for high-economic fish such as tuna (Teliandi *et al*., 2013). MLD also plays an important role in near-surface acoustic propagation (Sutton *et al*., 2014). In addition, the surface layer of the oceans stores heat which is a source of global fluctuations such as El Niño (Guan *et al*., 2019).

MLD is commonly determined from temperature, salinity, and density profiles (via temperature-salinity calculations) (Rath *et al*., 2016). MLD varies temporally from diurnal (Ushijima and Yoshikawa, 2019), intra-seasonal and annual (Holte and Talley, 2009), to inter-annually caused by various things such as surface forces, lateral advection, internal waves and so on (Montégut *et al*., 2004). Indian Ocean waters has a significant influence on Indonesian waters, especially EIO. The EIO is quite complex because it is influenced by oceanographic and atmospheric phenomena, e.g., Indian Ocean Dipole (IOD) (Sun *et al*., 2019) and upwelling (Chen *et al*., 2016). MLD is an important parameter in the air-sea interaction system. In its role, MLD, which has a high thickness, exhibits a greater heat capacity. Consequently, this leads to a decrease in responsiveness to atmospheric heat flux, as deeper MLDs take longer to respond to atmospheric forcing. Seawater flux variations play an important role for global climate variations, especially the Indian Ocean. This variation in climate change could potentially trigger ecological disturbances such as coral bleaching in the waters of West Sumatra which directly borders the EIO (Wisha *et al*., 2021). Seawater flux is one of those responsible for the warming that occurs during ENSO in the Indian Ocean (Jin and Wright, 2020) and after the end event of ENSO (Xie *et al*., 2010). In addition, depending on the season and location, it can contribute positively or negatively to IOD growth. (Qiu *et al*., 2014; Lu *et al*., 2018). The Indian Ocean also responds to the Pacific phenomenon as a process of teleconnections. This teleconnection is associated with El Niño activity in the Pacific, commonly causing warming in the Indian Ocean. (Yuan *et al*., 2018). In their research Carton *et al*. (2008) explained that atmospheric teleconnections that occurred during El Niño events caused MLD siltation in the eastern equatorial Indian Ocean and deepened south of the equator.

However, previous studies have focused on certain parts of the time and space scales that are separated from one variability to another. To the best of our knowledge, very few studies have been conducted on the full range of variability including the presence of extreme (positive and negative) IOD. From some of the descriptions above, we consider it necessary to study and understand the dynamics of fluctuation of the MLD related to the Indian Ocean climate mode. The aim of this research is to specify the variability of MLD in the EIO (West Sumatra) using observational data. This study attempts to understand the 3-month (intra-seasonal) average MLD variability in relation to sea surface properties, especially with Sea Surface Temperature (SST) and wind as the preeminent driving force by considering the IOD phenomenon. It is a key parameter in the atmosphere-ocean heat exchange and climate regulation.

2. Materials and Methods

2.1 Material

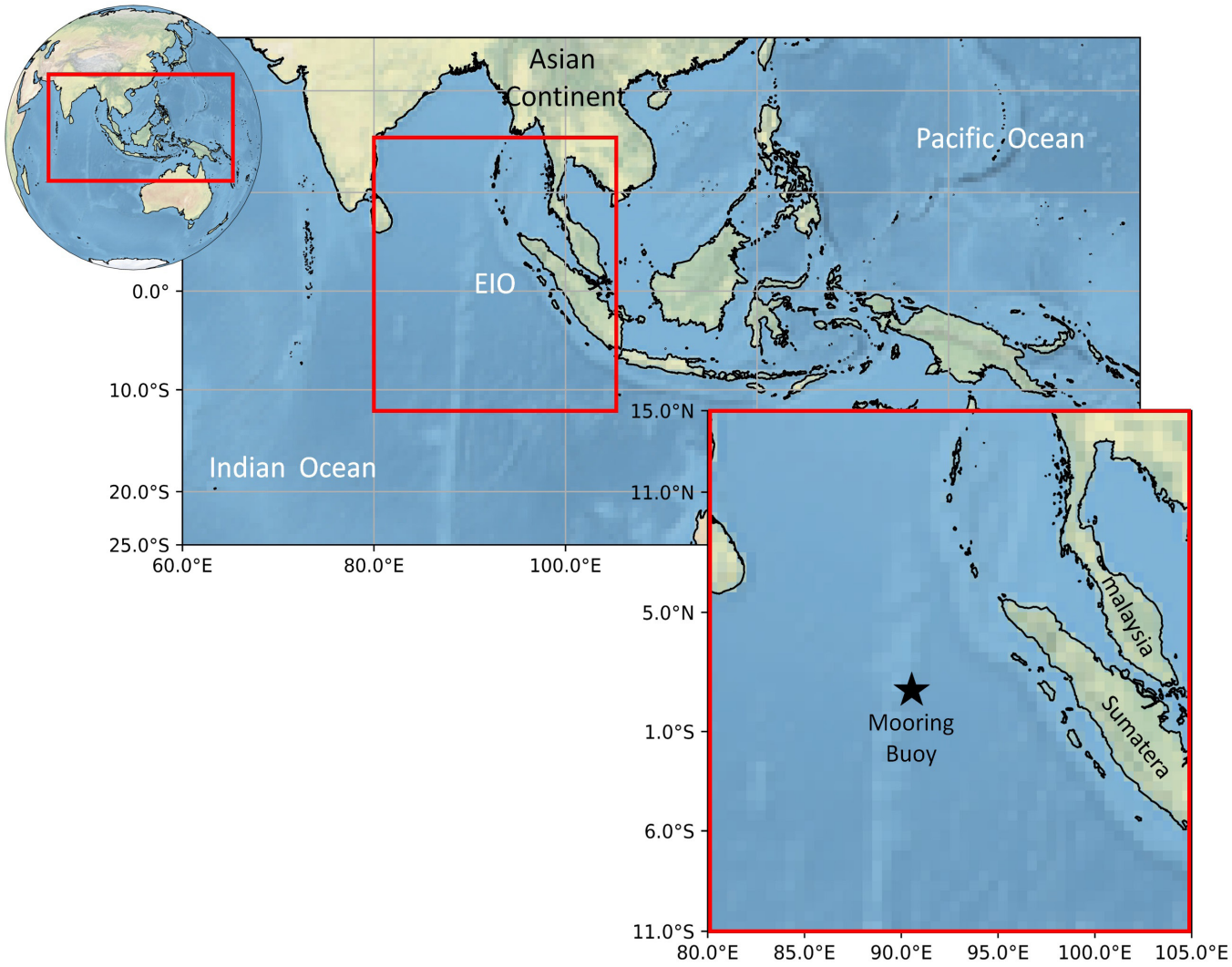

Figure 1. Geographical and bathymetric maps of the region around the maritime continent of Indonesia. Globe map on the upper right to mark the magnification of the map of the research location area. The research location is in the eastern Indian Ocean which is indicated by a box shape with a red dotted line. The black star is the point for time series analysis. This research location covers the equator and low latitude areas.

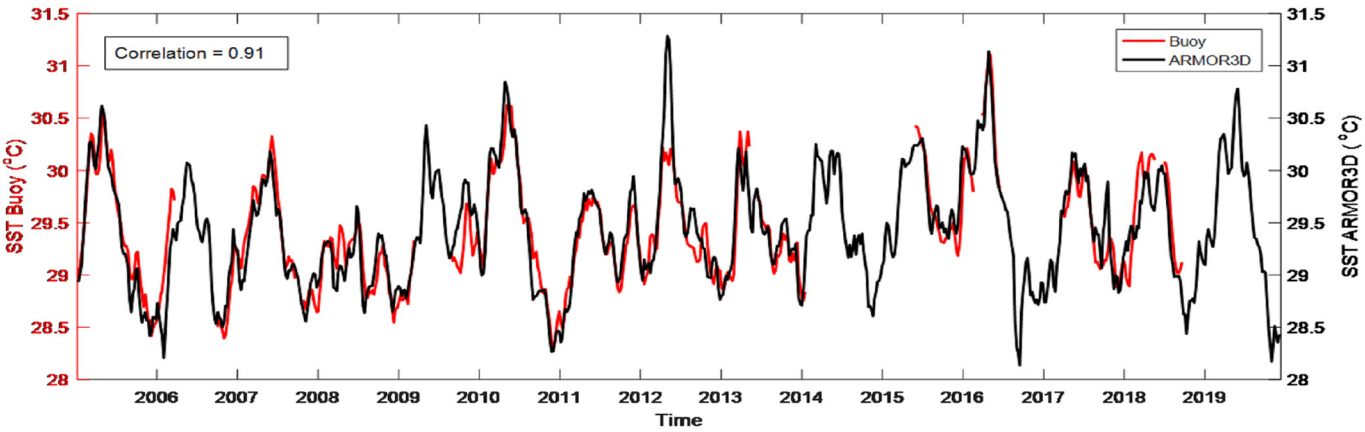

Figure 2. Comparison of SST values between ARMOR3D and Buoy. The red line is for the SST Buoy value and the black line is for the ARMOR3D SST value with the same temperature scale range.

This research is in the eastern Indian Ocean with coordinates 80°E – 105°E and 16.5°N – 11.5°S which are directly adjacent to the Bay of Bengal in the north and Sumatra Island in the east (Figure 1). The data used is weekly Mixed Layer Depth (MLD) from 1998 to 2020 from ARMOR3D which can be accessed on the http://marine.copernicus.eu/ page. ARMOR3D data is a combination of in-situ (Temperature and Salinity observations) and real data satellite using statistical methods on a 1/4◦ horizontal regular grid with 33 layers with unevenly spaced between surface layers up to 5.500 m depth (Guinehut *et al*., 2012; Mulet *et al*., 2012; Le Traon *et al*., 2017). The MLD in this dataset is the depth when the potential density anomaly (sigma-theta) is 0.05 Kg/m^3 which is equivalent to a threshold of 0.2°C for temperature. This MLD determination is in accordance with the threshold temperature criteria by Montégut *et al*. (2004).

$$MLD = \text{depth where } T = T10m \pm 0.2°C \ldots\ldots (1)$$

Where T is temperature.

In determining the criteria variable density corresponds to a variation of 0.2 °C where in climatological procedures it is still capable of being an appropriate estimator compared to other variations (0.5°C (Levitus, 1982) and 0.8°C (Kara *et al*., 2000) at local temperature conditions from a depth of 10 meters .

$$MLD = \text{depth where } \sigma 0 = \sigma 010m + \Delta\sigma 0 \ldots\ldots (2)$$

with $\Delta\sigma 0 = \sigma 0\ (\theta 10m - 0.2°C, S10m, P0) - \sigma 0\ (\theta 10m, S10m, P0)$.

The final result of the calculation on ARMOR3d is that MLD is defined as the minimum MLD which is calculated from the density criteria and MLD which is determined from the temperature criteria. On two criteria, namely density and temperature, MLD produces a linear interpolation to the depth where the threshold is reached. This determination has been used in a study by Wade *et al*. (2011) also based on the numerical model input that has been done by Keerthi *et al*. (2013).

As validation, we use a Rama buoy moored in the EIO. The data set for RAMA buoys consists of 23 moored buoys spread across and operating in the basin of Indian Ocean (McPhaden *et al*., 2009) (http://www.pmel.noaa.gov/tao/rama). Objectively selecting a buoy that is right on the equator at 90°E is chosen to be used in this study. The selection of this one buoy is based on data continuity which has significantly higher temporal resolution when compared to other RAMA buoys. Furthermore, the site was chosen because it lies in a region related to the dynamics of air-sea interactions such as the Madden–Julian Oscillation (MJO) (Matthews, 2008; Yoneyama *et al*., 2013), Indian Ocean Dipole (IOD) (Zhang *et al*., 2015; Wainwright *et al*., 2020), monsoon (Abish, 2013; Annamalai, 2013), affected by ENSO (Baquero-Bernal *et al*., 2002; Zhao *et al*., 2019) as well as other variability. In general, the floats at coordinates 0°, 90°E have the greatest amount of high-resolution data and this is necessary for calculating or validating data.

The interannual climate variability index used for data for 1998-2020 is the Dipole Mode Index (DMI) with monthly intervals that occur in the Indian Ocean. This is used to see climate variability that affects oceanographic conditions in the study area in that range of years. DMI were collected from the National Oceanic and Atmospheric Administration (NOAA), which can be accessed at: https://psl.noaa.gov/gcos_wgsp/Timeseries/Data/dmieast.had.long.data. Wind data descriptions were used to analyze climatology in the EIO from the European Center for Medium-Range Weather Forecasting (ECMWF) Reanalysis v5 (ERA5), data were captured online (https://cds.climate.copernicus.eu/).

2.2 Method

In this study time series data will be analyzed. Analysis using the Continuous Wavelet Transform (CWT) method is used to test power variations in data in the form of long time series data (Torrence and Compo, 1998). This data allows determining the main periodicity from its variability and fluctuation (Grinsted *et al*., 2004; Bendat and Piersol, 2010; Emery and Thomson, 2014). In this study, CWT analysis was performed on MLD time series data using Morlet wavelets, so the formula can be written as:

$$W_n^X(s) = \sqrt{\frac{\delta t}{s}} \sum_{n'=1}^{N} x_n, \psi o \left[\frac{(n'-n)\delta t}{s}\right] \ldots\ldots (3)$$

Where s is the wavelet variation scale, at $x_n\ x_n$, nn=1, . ., N is a time series, $\delta t\delta t$ is a uniform time interval and $\psi 0\psi 0$ is a dimensionless frequency.

In addition, this study also uses the Cross-Continuous Wavelet Transform (XWT) analysis method which is applied to SST and MLD data as X and Y. So based on Torrence and Webster (1999) formula it can be written as follows:

$$R_n^2(s) = \frac{\left|\left(s^{-1} W_n^{XY}(s)\right)\right|^2}{\left(s^{-1}\left|W_n^X(s)\right|^2\right)\left(s^{-1}\left|W_n^Y(s)\right|^2\right)} \ldots\ldots (4)$$

Then a bandpass filter was performed in the

seasonal and interannual periods for analysis. Bandpass is performed using a Butterworth filter which has an output value is then used as input (recursively) in the frequency domain so as not to change the amplitude of the filtered signal. Bandpass for interannual variability is in the 2-7 years period. The observations used in this study used ARMOR3D data which will then be explained as follows. To validate the Sea Surface Temperature data, this study uses Sea Surface Temperature data observed from the Buoy mooring points in the Indian Ocean (Figure 1) with the same time range as ARMOR3D data with some data gaps. The sea surface temperature data from ARMOR3D agrees significantly with the buoy data. Comparison of sea surface temperature values ARMOR3D-Buoy has a fairly good correlation coefficient with a value of 0.91 (Figure 2).

3. Results and Discussion

3.1 General Condition

In order to expose the main period of MLD depth, wavelet strength spectra of the MLD data on ARMOR3D records were calculated. Wavelet analysis of MLD data at point 90E, 0 from 1998-2018 showed variability that varies from intra-season, semi-annual, annual, to interannual (2.5-3 years) (Figure 3). The annual (seasonal) variability is related to monsoons while the 2.5 years interannual fluctuation is associated to the IOD which looks quite significant (red color with black contour). The black line with a white fill in the image represents the 95% confidence level. This is as described using the application of a numerical model and direct observation by Keerthi *et al.* (2013). Indian Ocean has very significant MLD fluctuations on an annual basis. The IOD can be interpreted as a mode of interannual variability in the tropical Indian Ocean resulting from positive interactions between the ocean and atmosphere. Saji *et al.* (1999) explained that most interannual variability in MLD are near the equator. The highly significant variability on the intra-seasonal and inter-annual time scales has also been illustrated by the study of Schott *et al.* (2009). Apart from that, the Indian Ocean also has a seasonal cycle with quite a large amplitude. This is related to the existence of reversed monsoon circulation (Schott *et al.*, 2002).

The MLD and SST time series data have no data gaps. these MLD and SST data were then analyzed using wavelet coherence (Figure 4). MLD depths ranged from approximately 20m to nearly 80m in mid to late 2016 (Figure 4a). The depth of the MLD experiences quite dynamic fluctuations following the effects of the sea-air interaction it receives. MLD relates to the field of wind pressure modulated by heat fluxes as well as fresh water mainly close to equator and parts of the northern Indian Ocean. During the significant active Southwest Monsoon period, Schott and McCreary (2001) described along the coastal of Somalia and the Arabian Sea wind-induced turbulent mixing and upwelling resulting in differences in the annual mean MLD depth in the western Arabian Sea in the ranges 50 – 60m. The relationship between the depth of MLD and SST is quite close. The MLD layer is an important variable in the ocean-atmosphere interaction process. Shinoda and Hendon (1998) explained that shallow MLD layers can refer to a decrease in thermal capacity. This will be able to encourage a significant SST temperature anomaly.

These SST variations are related to feedback on intra-seasonal variations in the atmospheric system, so it is important to study the processes that drive these SST variations (Matthews, 2004; Bellenger and Duvel, 2009). SST time series data show clear intra-seasonal fluctuations. For one year, several peaks and valleys were observed which fluctuated with a minimum valley value range of 28.2°C in mid-2001 and a maximum peak value of 30.7°C in mid-2016 (Figure 4b). The intra-seasonal variability of SST and MLD in general has been studied especially in the Indian Ocean. The observed SST intra-seasonal fluctuations or signals are related to the MLD intra-seasonal signals. Drushka *et al.* (2014) compiled Argo's data and estimated MLD fluctuations in response to forces from intra-seasonal variability. The coherence between SST and MLD shows a strong correlation in the monsoon period (one year) and the Indian Ocean Dipole (2-3 years). In the annual period, changes in SST respond more quickly than MLD. This can be seen from the SST phase preceding the MLD phase by 30-90 degrees. This also occurs during the IOD period where SST responds more quickly to changes in MLD. This is because the change in SST only covers the surface layer while the mixed layer will take time for mixing to occur.

3.2 Seasonal Variability

Several studies have investigated the seasonal variation of Indian Ocean MLD. In this study found that in the southern part of equator there is a significant difference in seasonal variations. Previous research by Schott *et al.* (2002) found that there is a significant semi-annual variation in MLD in northern Indian Ocean which is linked to the monsoon circulation that occurs seasonally. Seasonal variation of MLD in the eastern Indian Ocean is defined by deep MLD depth in JJA-SON and low in DJF-MAM. In JJA-SON, the maximum mixed layer depth (MLD) is observed to be significantly deeper in the southern region, ranging from 35 to 75 meters, as compared to the northern region,

which exhibits a shallower range of 20 to 40 meters (Figure 5). The Eastern North Indian Ocean appears to have a shallower MLD. This is related to counteracting the stabilizing effect of intense freshwater flux experienced by the Bay of Bengal during the summer monsoon. (Shenoi *et al*., 2002). Whereas in the south of the equator, the MLD is significantly influenced by climatological wind magnitude, so it has a deeper MLD around 10°S that the easterly winds are significant. These results agree with the model built to reproduce large-scale MLD structures fairly well by Keerthi *et al.* (2013). This shows that the MLD layer is influenced by seasonal conditions. Wyrtki (1961) also explained that the MLD variation is caused by the movement of water masses and the change of monsoons.

The Gulf of Thailand, which is behind the peninsula of Malaysia, shows a data gap. Previous research by Keerthi *et al.* (2013) used a model to simulate MLD which is shallower than direct observations in coastal areas. This may arise due to Argo's lack of profile in the region causing uncertainty in the MLD calculations (Nisha *et al*., 2013). This model also found that the MLD is shallower onward the equator that may be related to a lack of atmospheric forces or a vertical mixing scheme. In general, in each season, the MLD value at the equator is higher than in other regions. At the equator, the MLD variation is more complex because what influences it is not just one dimension but can also be three dimensions such as the rise of the thermocline layer due to Kelvin waves or due to upwelling by Ekman. During winter season, snowfall occurs, and radiation of solar weakens. This makes the Asian continent colder and causes high stress on the continent to build up. This causes northerly winds from the continents to push dry and cold air masses over the Indian Ocean toward the equator line (de Laat and Lelieveld, 2002).

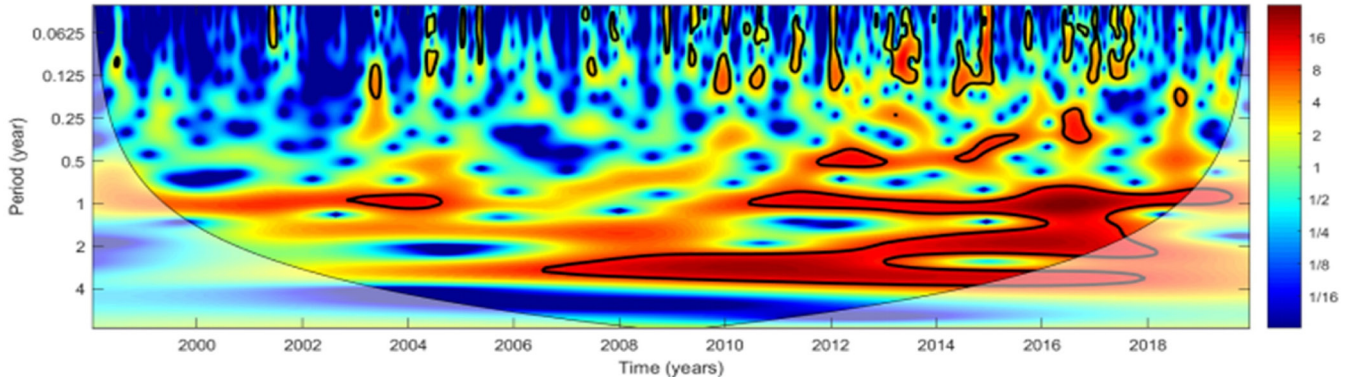

Figure 3. MLD data wavelet transform at point 90E, 0N. Period is written in annual terms, the value is > 1 for Interannual Variability (IV), 1 for Annual Variability (AV), 0.5 for Semiannual Variability (SAV).

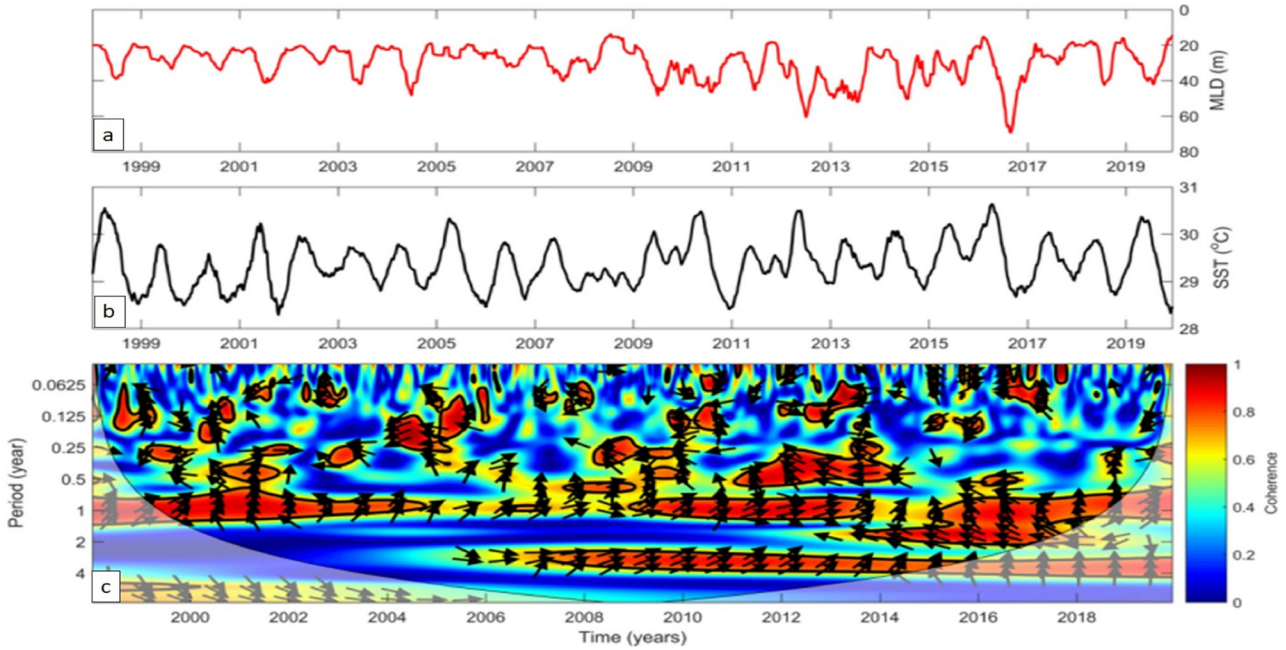

Figure 4. Timeseries (a) MLD and (b) SST at point 90°E, 0. (c) The right arrow on the coherence wavelet indicates that the two timeseries are in phase while the arrow to the left is anti-phase, the arrow up indicates that the SST phase precedes MLD as far as 90°

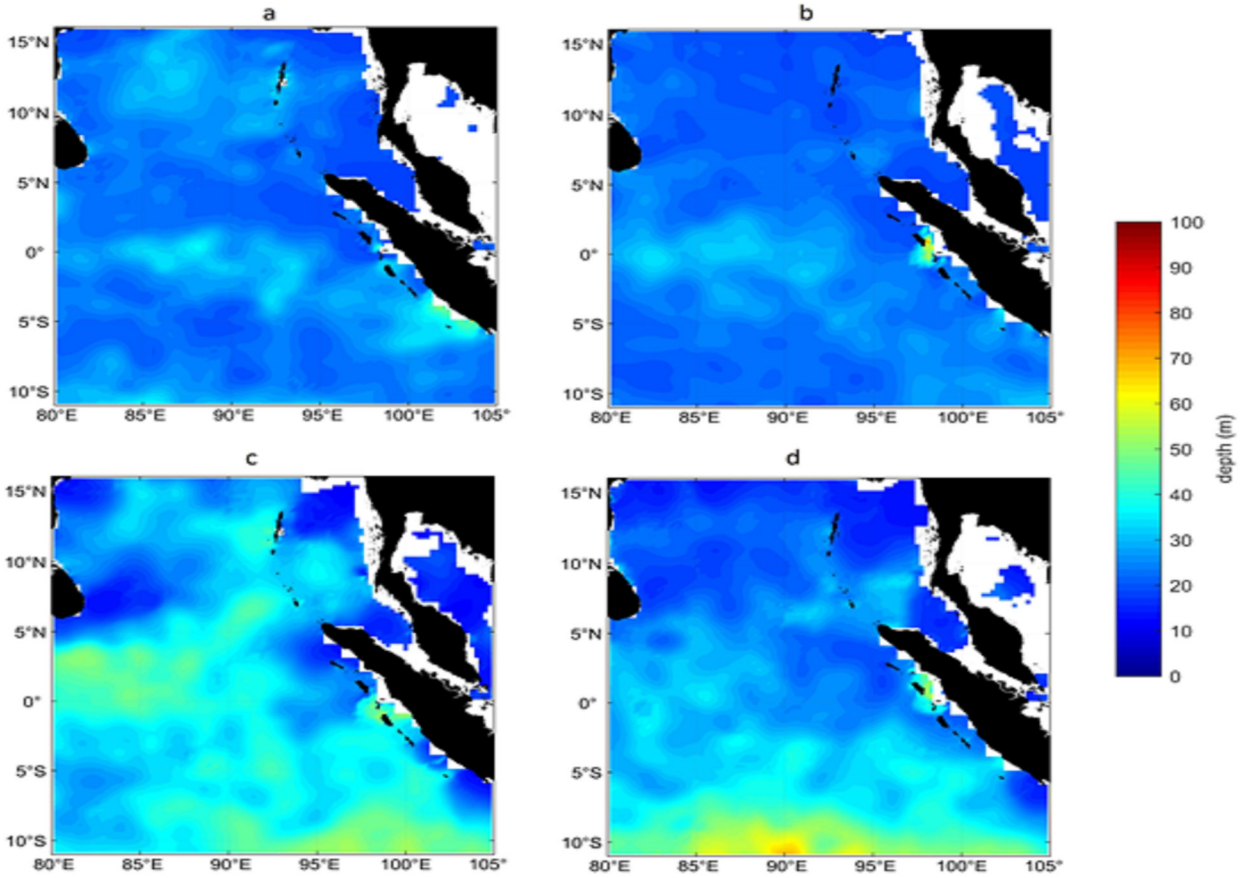

Figure 5. MLD 3-month climatological average: a. December-January-February (DJF); b. March-April-May (MAM); c. July-July-August (JJA); d. September-October-November (SON). Bar scale applies to all images.

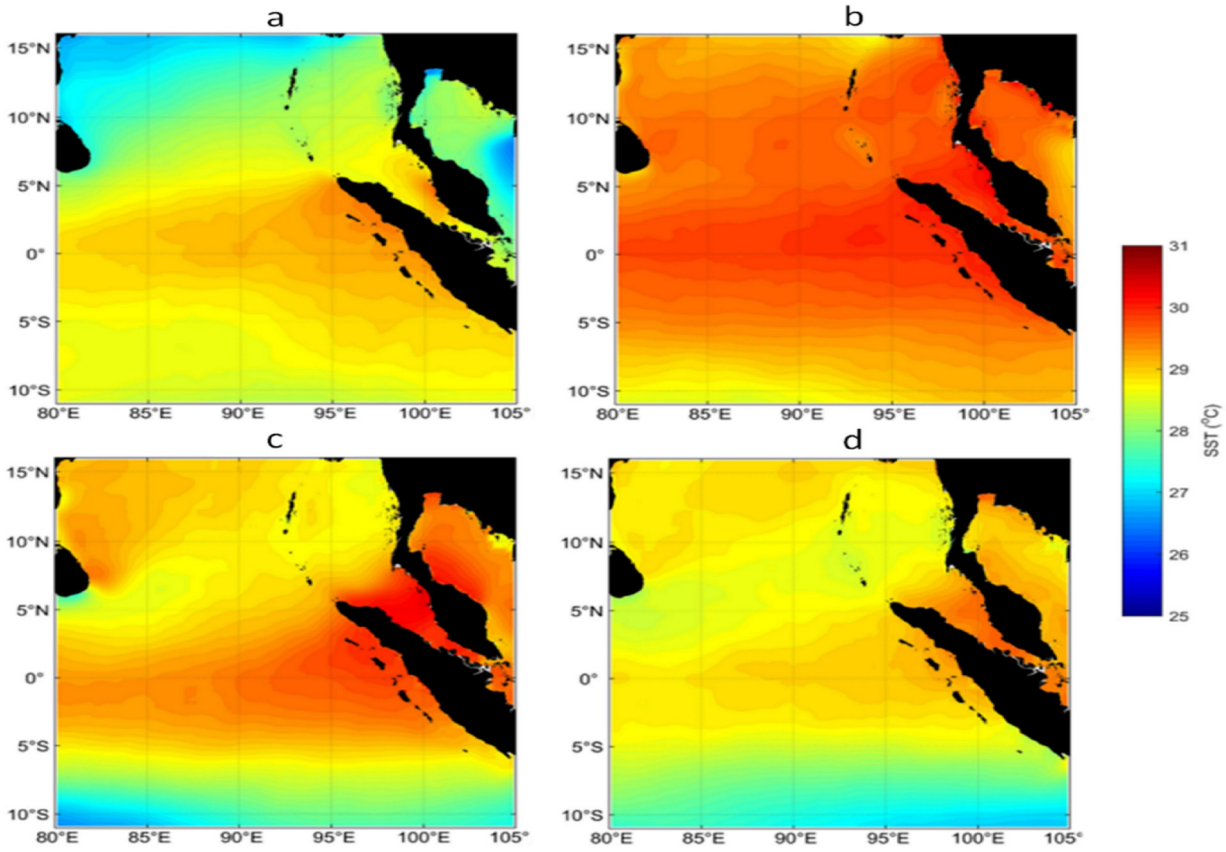

Figure 6. SST 3-month climatological average: a. December-January-February (DJF); b. March-April-May (MAM); c. July-July-August (JJA); d. September-October-November (SON). Bar scale applies to all images.

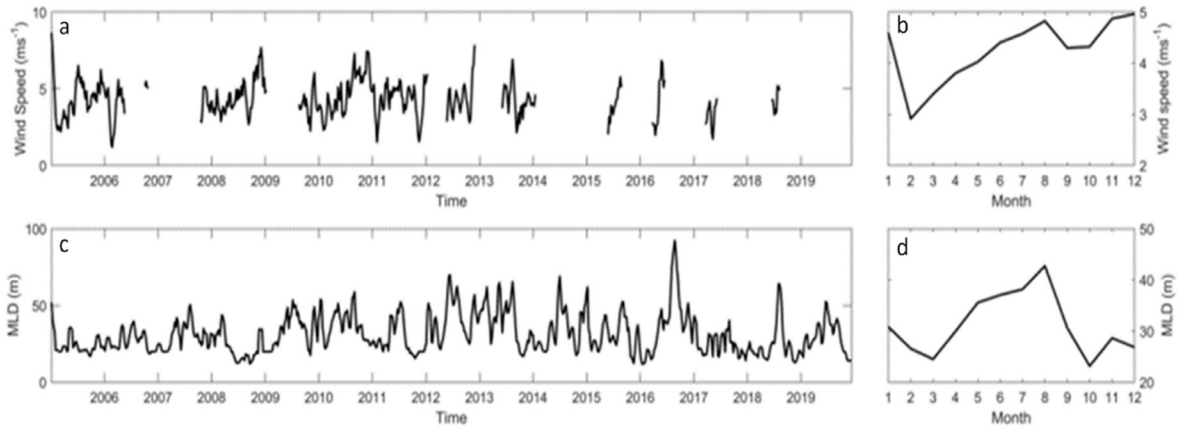

Figure 7. Graph of time series and monthly climatology data. (a) wind speed time series and (b) monthly climatology wind speed. (c) MLD time series and (d) monthly climatology MLD.

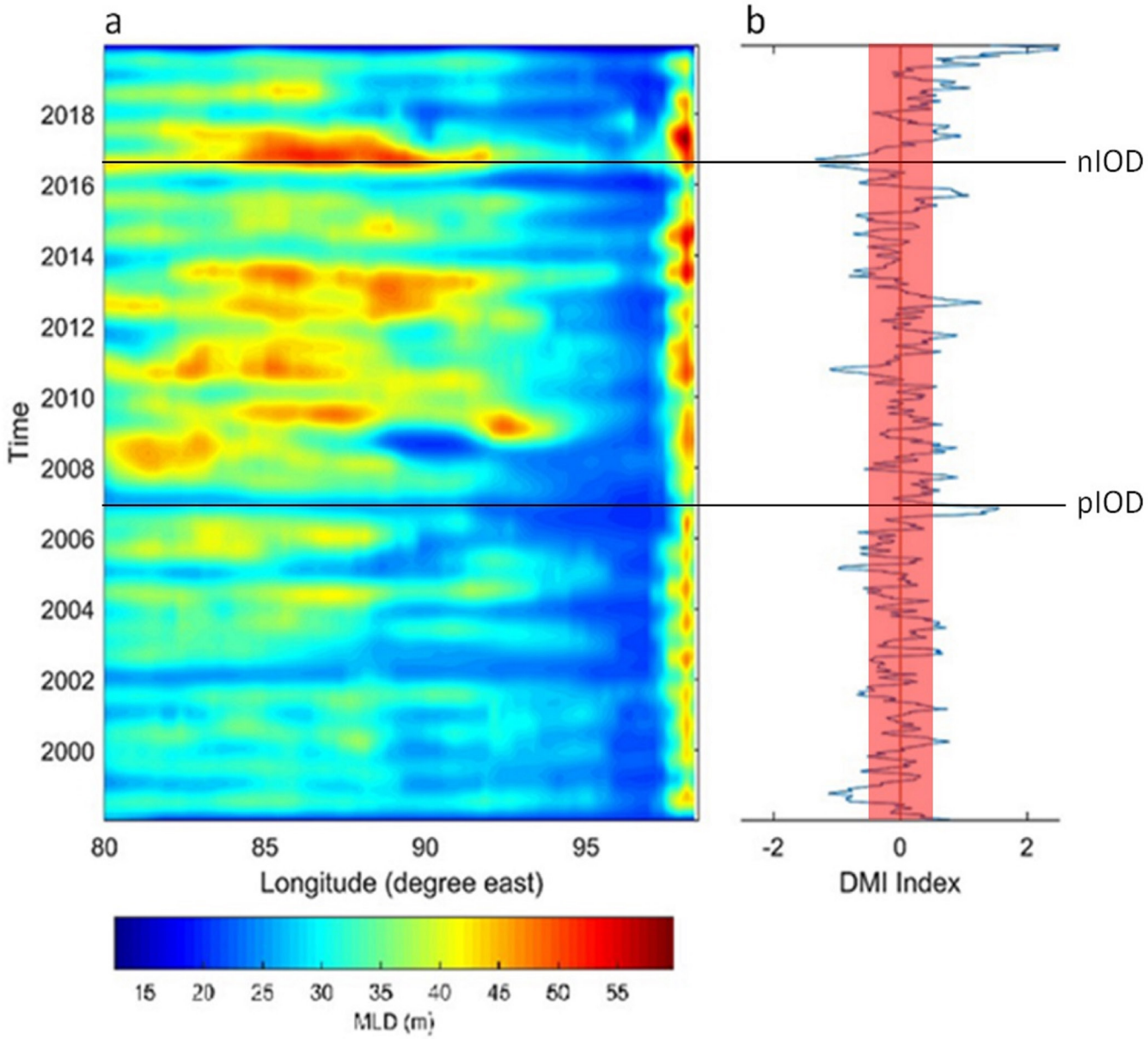

Figure 8. (a) Hovmoller diagram of MLD at the equator from 1998-2020 at longitude 80-105oE. (b) The DMI index with a transparent red threshold. Description nIOD for negative and pIOD for positive.

MLD thickness is able to modulate its heat capacity. Because such a response makes MLD tend to be heated or cooled by the forces acting, especially active atmospheric forces such as IOD and ENSO. In line with this, MLD is a parameter that plays a crucial role in ocean-atmosphere interactions. This is because MLD is able to modulate the response amplitude of SST. The minimum value of the MLD corresponds to the maximum temperature value (Figure 6). The high SST value causes effective evaporation of sea water which results in high rainfall. This is caused by the Monsoon Intra-seasonal Oscillation (MISO). According to Girishkumar *et al*. (2017), MISO significantly affects seasonal variability in the EIO (near the Bay of Bengal). The DJF-MAM month (Figure 6a, 6b) generally has a higher SST when compared to the JJA-SON month (Figure 6c, 6d) based on the spatial distribution. The maximum SST is distributed almost evenly and reaches a peak in MAM and then gradually decreases in JJA-SON and low SST appears south of the equator. Climatology showed a different response every three months. Atmospheric heat flux acting on waters is possible to become the dominant process that is able to promote intra-seasonal variability as a response to the active phase of monsoon variability (Waliser *et al*., 2004).

The Indian Ocean is dominated by strong winds throughout the year by two periods, namely, the northeast monsoon period and the southwest monsoon period. Strong seasonal variability predominates in determining MLD. The determination of MLD is dominated by surface winds and sensible and latent heat fluxes in Indian Ocean, especially in Arabian Sea (Bauer *et al*., 1991). This study obtains a pattern that is bound between wind speed and MLD and related to wind speed conditions (Figure 7). The wind climatological pattern and the MLD pattern are the same, namely high in August. In the southern part of the equator, MLD is more inclined to be driven by significant climatological wind intensity. This can be seen from the MLD response, which is deeper, where the east wind is the strongest. The seasonal shallowing and deepening of the MLD in the southwest Indian Ocean are associated with annual wind cycles. This process is caused by the effect of wind movement and its effect on buoyancy flux and depth of thermocline (Foltz *et al*., 2010).

3.3 Interannual Variability

The Indian Ocean is known to be able to respond to interannual variations triggered by remote ENSO influences. The sea-air interaction that works when ENSO is active makes it possible to have an SST anomaly impact. This process will also have an impact on climate and this influence can persist in the Indian Ocean long after El Niño events ends (Xie *et al*., 2010). Furthermore, the Indian Ocean also has its own mode or commonly called the IOD. IOD is characterized as an active ENSO phase in the Pacific Ocean, which is the impact of ocean-atmosphere interaction processes. IOD at its peak during autumn, this is associated with an eastern anomaly in the middle of the Indian Ocean, an SST anomaly with low SST seen around the islands of Java and Sumatra and an SST anomaly with warmer temperatures in the western Indian Ocean.

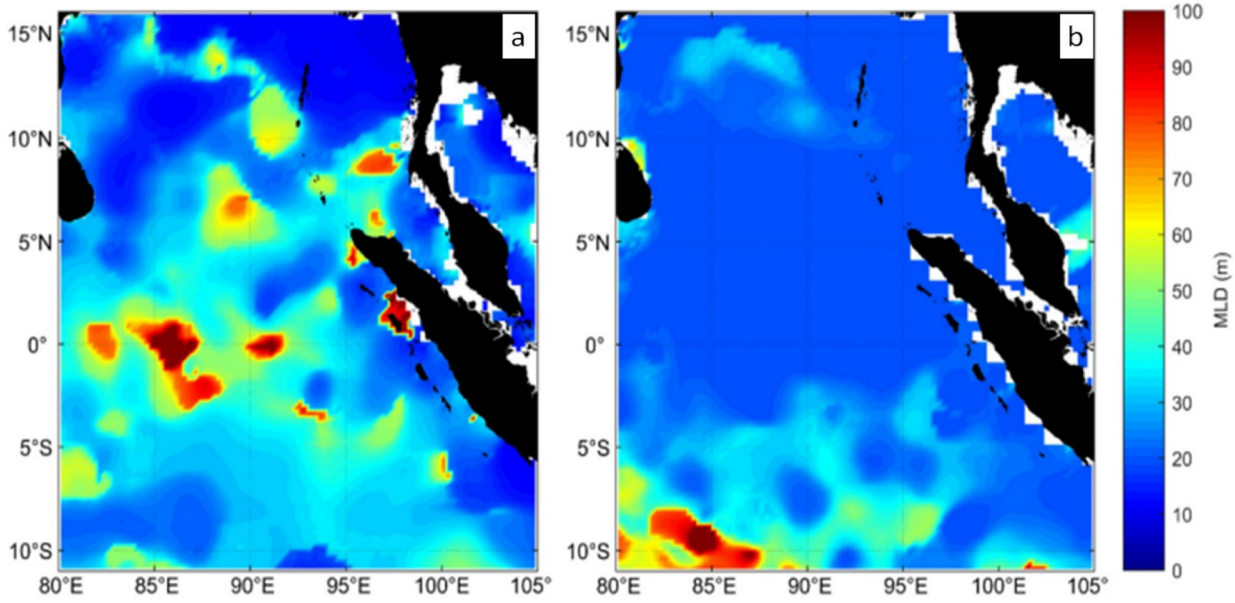

Figure 9. MLD conditions during strong IOD events: (a) nIOD in September 2016 and (b) pIOD in November 2006

This is as revealed by the research of Webster *et al.* (1999) on the air-sea coupling in the Indian Ocean. The existence of teleconnections that occur is increasingly felt because there is a strong tendency that an active El Niño event triggers IOD, but it is also possible for the two events to occur independently (Annamalai *et al.*, 2003).

To fully see the state of MLD on a time scale based on longitude, Hovmoller was used. There is a significant response for each DMI index value at MLD depth. IOD is described by the dipole mode index (DMI) (Saji *et al.*, 1999). This index shows how strong the value and intensity are. To determine this, the definition from Ummenhofer *et al.* (2009) classification for conducting composites for IOD/ENSO in the Indian Ocean. A robust IOD is definite as a year when an anomaly occurs which is normalized to be greater than 0.5, so if it is below 0.5 it is considered normal. Hovmoller variability of MLD at 0 degrees latitude at longitude 80 to 105 east longitude shows that when nIOD occurs, MLD is continuously and clearly higher than when pIOD has lower MLD (Figure 8). The most obvious example is when the nIOD was strong at the end of 2016. Meanwhile, the MLD under pIOD conditions was relatively shallow, such as at the end of 2019 and 2007. The area around the island has a stronger response to IOD, as seen from the MLD value which is deeper than other areas (Figure 9).

Spatially, the negative IOD is strong, and the mixed layer depth is relatively high in the equatorial regions, in the north, and near the coast of Sumatra. In contrast, when a robust positive IOD occurs, the MLD is very deep in the south (at latitude 5 degrees to the south), while in the equator, north and the coast over the west coast of Sumatra, the depth of the MLD is very shallow. IOD, like ENSO, is the result of ocean-atmosphere interactions. IOD peaks in autumn and is associated with the northeastern central Indian Ocean anomaly, the cold SST anomaly near Java and Sumatra, and the warm SST anomaly in the western Indian Ocean. (Saji *et al.*, 1999; Webster *et al.*, 1999; Murtugudde *et al.*, 2000). Shallow MLD causes a small ocean heat storage capacity, causing sea surface temperatures to rise resulting in atmospheric convection (Keerthi *et al.*, 2015).

4. Conclusion

Wavelet analysis of MLD data at point 90E, 0 from 1998-2018 shows variability that varies from intra-seasonal, semi-annual, annual to interannual (2.5-3 years). MLD depths ranged from approx. 20m to nearly 80m in the mid to late 2016 period. The SST and MLD time series data show quite pronounced intra-seasonal fluctuations. The observed SST intra-seasonal fluctuations or signals are related to the MLD intra-seasonal signals. Seasonal variation of MLD in the EIO is characterized by deep MLD depth in JJA-SON and low in DJF-MAM. In JJA-SON, the maximum MLD depth is found to be deeper in the south than in the north. Spatially the MLD in the south of the equator is deeper than in the north. Interannually, MLD is heavily influenced by the IOD. When the nIOD occurs, the MLD is continuously and clearly higher than when the pIOD has a lower MLD. MLD depth is deeper in nIOD with a maximum depth in the range of 100 m compared to pIOD in the range of 20 m around the equator. MLD with maximum depth in the strong nIOD phase is around the equator and the pIOD phase is south of the equator. This study also shows that the interannual variability of the area around the mainland has a stronger response.

Acknowledgement

We thank the reviewers and technical editor for advice and comments on the initial version of this manuscript. This research is based on the Copernicus—Marine environment monitoring service products (http://marine.copernicus.eu/). RAMA buoy in action at the equator of the Indian Ocean (http://www.pmel.noaa.gov/tao/rama). DMI were collected from the National Oceanic and Atmospheric Administration (NOAA), which can be accessed at: https://psl.noaa.gov/gcos_wgsp/Timeseries/Data/dmieast.had.long.data. Wind surface data from the European Center for Medium-Range Weather Forecasting ERA5 data were obtained online (https://cds.climate.copernicus.eu/).

Authors' Contributions

The contribution of each author is as follows, RF; collected and visualized the data, and drafted the manuscript. AYY; provided concept, improved manuscript, and revised the manuscript critically. AYY and RF; discussed the analysis of the data results. All authors discussed and contributed to the final manuscript.

Conflict of Interest

This research does not receive grants in general or specifically from any funding agency, whether in the government, public, commercial, or non-profit sector.

Funding Information

This research has no funding.

References

Abdulla, C. P., Alsaafani, M. A., Alraddadi, T. M., &

Albarakati, A. M. (2016). Estimation of mixed layer depth in the Gulf of Aden: A new approach. *PLoS ONE*, 11(10)1-16.

Abdulla, C. P., Alsaafani, M. A., Alraddadi, T. M., & Albarakati, A. M. (2018). Mixed layer depth variability in the Red Sea. *Ocean Science*, 14(4):563–573.

Abish, B., Joseph, P. V., & Johannessen, O. M. (2013). Weakening trend of the tropical easterly jet stream of the boreal summer Monsoon Season 1950–2009. *Journal of Climate*, 26:9408-9414.

Annamalai, H., Hafner, J., Sooraj, K. P., & Pillai, P. (2013). Global warming shifts the monsoon circulation drying South Asia. *Journal of Climate*, 26:2701-2718.

Annamalai, H., Murtugudae, R., Potemra, J., Xiea, S. P., Liu, P., & Wang, B. (2003). Coupled dynamics over the Indian Ocean: Spring initiation of the Zonal Mode. *Deep Sea Research Part II: Tropical Studies in Oceanography*, 50(12-13):2305-2330.

Baquero-Bernal, A., Latif, M., & Legutke, S. (2002). On Dipolelike variability of sea surface temperature in the tropical Indian Ocean. *Journal of Climate*, 15:1358-1368.

Bauer, S., Hitchcock, G. L., & Olson, D. B. (1991). Influence of monsoonallyforced Ekman dynamics upon surface layer depth and plankton biomass distribution in the Arabian Sea. *Deep Sea Research Part A. Oceanographic Research Papers*, 38(5):531-553.

Bellenger, H., & Duvel, J. P. (2009). An analysis of tropical ocean diurnal warm layers. *Journal of Climate*, 22:3629-3646.

Bendat, J. S., & Piersol, A. G. (2010). Random data: Analysis and measurement procedure. Canada: John Wiley and Sons Inc.

Besa, I., Makaoui, A., Hilmi, K., & Afifi, M. (2018). Variability of mixed layer depth and the ocean surface properties in the Cape Ghir region, Morocco for the period 2002-2014. *Modeling Earth System and Environment*, 4:151-160.

Carton, J. A., Grodsky, S. A., & Liu, H. (2008). Variability of the oceanic mixed layer 1960-2004. *Journal of Climate*, 21:1029-1047.

Chen, G., Han, W., Li, Y., & Wang, D. (2016). Interannual variability of equatorial Eastern Indian Ocean upwelling: Local versus remote forcing, *Journal of Physical Oceanography*, 46(3):789-807.

de Laat, A. T. J., & Lelieveld, J. (2002). Interannual variability of the Indian winter monsoon circulation and consequences for pollution levels. *Journal of Geophysical Research: Atmospheres*, 107(D24):ACH 2-1–ACH 2-13.

Drushka, K., Sprintall, J., & Gille, S. T. (2014). Subseasonal variations in salinity and barrier-layer thickness in the eastern equatorial Indian Ocean. *Journal of Geophysical Research*, 119(2):805-823.

Emery, W. J., & Thomson, R. E. (2014). Data analysis methods in physical oceanography (3rd Ed). Massachusetts: Elsevier.

Foltz, G. R., Vialard, J., Kumar, B. P., & McPhaden, M. J. (2010). Seasonal mixed layer heat balance of the southwestern tropical Indian Ocean. *Journal of Climate*, 23:947-965.

Girishkumar, M. S., Joseph, J., Thangaprakash, V. P., Pottapinjara, V., & McPhaden, M. J. (2017). Mixed layer temperature budget for the northward propagating summer monsoon intraseasonal oscillation (MISO) in the Central Bay of Bengal. *Journal Geophysical Research: Oceans*, 122:8841-8854.

Grinsted, A., Moore, J. C., & Javreja. S. (2004). Application of cross wavelet transform and wavelet coherence to geophysical time series. *Nonlinear Processes in Geophysics*, 11(5/6):561-566.

Guan, C., Hu, S., McPhaden, M. J., Wang, F., Gao, S., & Hou, Y. (2019). Dipole structure of mixed layer salinity in response to El Niño-La Niña asymmetry in the tropical Pacific. *Geophysical Research Letters*, 46(21):12165-12172.

Guinehut, S., Dhomps, A. L., Larnicol, G., & Le Traon, P. Y. (2012). High resolution 3-D temperature and salinity fields derived from in situ and satellite observation. *Ocean Science*, 8:845-857.

Holte, J., & Talley, L. (2009). A new algorithm for finding mixed layer depths with applications

to argo data and subantarctic mode water formation. *Journal of Atmospheric and Oceanic Technology*, 26:1920-1939.

Itoh, S., Yasuda, I., Saito, H., Tsuda, A., & Komatsu, K. (2015). Mixed layer depth and chlorophyll a: Profiling float observations in the Kuroshio–Oyashio Extension region. *Journal of Marine Systems*, 151:1-14.

Jin, X., & Wright, J. S. (2020). Contributions of Indonesian throughflow to eastern Indian Ocean surface variability during ENSO events. *Atmospheric Science Letters*, 21(8):e979.

Kara, A. B., Rochford, P. A., & Hurlburt, H. E. (2000), An optimal definition for ocean mixed layer depth. *Journal of Geophysical Research: Oceans*, 105(C7):16803-16821.

Keerthi, M. G., Lengigne, M., Drushka, K., Vialard, J., Montégut, C. de B., Pous, S., Levy, M., & Muraleedharan, P. M. (2015). Intraseasonal variability of mixed layer depth in the tropical Indian Ocean. *Climate Dynamics*, 46:2633-2655.

Keerthi, M. G., Lengaigne, M., Vialard, J., Montégut, C. de B., & Muraleedharan, P. M. (2013). Interannual variability of the Tropical Indian Ocean mixed layer depth. *Climate Dynamics*, 40:743-759.

Le Traon, P. Y., Ali, A., Alvarez Fanjul, E., Aouf, L., Axell, L., Aznar, R., et al. (2017). The Copernicus marine environmental monitoring service: Main scientific achievements and future prospects. *Special Issue Mercator Ocean Journal*, 56:1-101.

Levitus, S. (1982). Climatological atlas of the world ocean (Vol. 13). US Department of Commerce: National Oceanic and Atmospheric Administration.

Lu, B., Ren, H. L., Scaife, A. A., Wu, J., Dunstone, N., Smith, D., Wan, J., Eade, R., MacLachlan, C., & Gordon, M. (2018). An extreme negative Indian Ocean Dipole event in 2016: Dynamics and predictability. *Climate Dynamics*, 51:89-100.

Matthews, A. J. (2004). The atmospheric response to observed intraseasonal tropical sea surface temperature anomalies. *Geophysical Research Letters*, 31(14):L14107.

Matthews, A. J. (2008). Primary and successive events in the Madden-Julian Oscillation. *Quarterly Journal of the Royal Meteorological Society*, 134(631):439-453.

McPhaden, M. J., Meyers, G., Ando, K., Masumoto, Y., Murty, V. S. N., Ravichandran, M., Syamsudin, F., Vialard, J., Yu, L., & Yu, W. (2009). RAMA: The research moored array for African-Asian-Australian monsoon analysis and prediction. *Bulletin of the American Meteorological Society*, 90:459-480.

Montégut, C. de B., G. Madec, A.S. Fischer, A. Lazar, & D. Iudicone. (2004). Mixed layer depth over global ocean: An examination of profile data and a profile-based climatology. *Journal of Geophysical Research: Oceans*, 109(C12).

Mulet, S., Rio, M. H., Mignot, A., Guinehut, S., & Morrow, R. (2012). A new estimate of the global 3D geostrophic ocean circulation based on satellite data and in-situ measurements. *Deep Sea Research Part II: Tropical Studies in Oceanography*, 77-80:70-81.

Murtugudde, R., McCreary Jr, J. P., & Busalacchi, A. J. (2000). Oceanic processes associated with anomalous events in the Indian Ocean with relevance to 1997-1998. *Journal of Geophysical Research*, 105(C2):3295-3306.

Nisha, K., Lengaigne, M., Vissa, G. V., Vialard, J., Pous, S., Peter, A. C., Durand, F., & Naik, S. (2013). Processes of summer intraseasonal sea surface temperature variability along the coasts of India. *Ocean Dynamics*, 63(4):329-346.

Qiu, Y., Cai, W., Guo, X., & Ng, Benjamin. (2014). The asymmetric influence of the positive and negative IOD events on China's rainfall. *Scientific Reports*, 4(4943).

Rao, R. R., & Sivakumar, R. (2000). Seasonal variability of near-surface thermal structure and heat budget of the mixed layer of the tropical Indian Ocean from a new global ocean temperature climatology. *Journal of Geophysical Research: Oceans*, 105:995-1015.

Rao, R. R., Molinari, R. L., & Fiesta, J. F. (1989). Evolution of climatological near-surface thermal structure of the tropical Indian Ocean: 1. Description of mean monthly mixed layer depth, and sea surface temperature, surface

currents and surface meteorological fields, *Journal of Geophysical Research: Oceans*, 94:10801-10815.

Rath, W., Dengler, M., Lüdke, J., Schmidtko, S., Schlundt, M., Brandt, P., Bumke, K., Marek, O., van der Plas, A. K., Junker, T., Mohrholz, V., Sarre, A., Tchipalanga, P. C. M., & Coelho, P. (2016). PREFCLIM: A high-resolution mixed-layer climatology of the eastern tropical Atlantic. *PANGAEA*.

Rugg, A., Foltz, G. R., & Perez, R. C. (2016). Role of mixed layer dynamics in tropical North Atlantic interannual sea surface temperature variability. *Journal of Climate*, 29:8083-8101.

Saji, N. H., Goswani, B. N., Vinayachandran, P. N., & Yamagata, T. (1999). A dipole mode in the tropical Indian Ocean. *Nature*, 401:360-363.

Schofield, O., Brown, M., Kohut, J., Nardelli, S., Saba, G., Waite, N., & Ducklow, H. (2018). Changes in the upper ocean mixed layer and phytoplankton productivity along the West Antarctic Peninsula. *Philosophical Transactions of the Royal Society A: Mathematical, Physical and Engineering Sciences*, 376(2122):20170173.

Schott, F. A., & McCreary, J. P. (2001). The monsoon circulation of the Indian Ocean. *Progress in Oceanography*, 51(1):1-123.

Schott, F. A., Dengler, M., & Schoenefeldt, R. (2002). The shallow overturning circulation of the Indian Ocean. *Progress in Oceanography*, 53(1):57-103.

Schott, F. A., Xie, S. P., & McCreary Jr, J. P. (2009). Indian Ocean circulation and climate variability. *Reviews of Geophysics*, 47(1):1-46.

Shenoi, S. S. C., Shankar, D., & Shetye S. R. (2002). Differences in heat budgets of the near-surface Arabian Sea and Bay of Bengal: Implications for the summer monsoon. *Journal of Geophysical Research*, 107(C6).

Shinoda, T., & H. H. Hendon. (1998). Mixed layer modeling of intraseasonal variability in the tropical Western Pacific and Indian Oceans. *Journal of Climate*, 11:2668–2685.

Smith Jr, W. O., & Jones, R. M. (2015). Vertical mixing, critical depths, and phytoplankton growth in the Ross Sea. *ICES Journal of Marine Science*, 72(6):1952-1960.

Sun, Q., Du, Y., Zhang, Y., Feng, M., Chowdary, J. S., Chi, J., Qiu, S., & Yu, W. (2019). Evolution of sea surface salinity anomalies in the Southwestern Tropical Indian Ocean during 2010-2011 Influenced by a Negative IOD Event. *Journal of Geophysical Research: Oceans*, 124(5):3428-3445.

Sutton, P. J., Worcester, P. F., Masters, G., Cornuelle, B. D., & Lynch, J. F. (2014). Ocean mixed layers and acoustic pulse propagation in the Greenland Sea. *The Journal of Acoustical Society of America*, 94:1517-1526.

Teliandi, D., Djunaedi, O. S., Purba, N. P., & Pranowo, W. S. (2013) Relationship between variability mixed layer depth $\Delta T=0.5^{o}C$ criterion and distribution of tuna in the eastern Indian Ocean. *Depik*, 2(3):162-171.

Torrence, C., & Compo, G. P. (1998). A practical guide to wavelet analysis. *Bulletin of the American Meteorological Society*, 79(1):61-78.

Torrence, C., & Webster, P. J. (1999). Interdecadal changes in the ENSO–Monsoon system. *Journal of Climate*, 12(8):2679-2690.

Ummenhofer, C. C., England, M. H., McIntosh, P. C., Meyers, G. A., Pook, M. J., Risbey, J. S., Gupta, A. S., & Taschetto, A. S. (2009). What causes southeast Australia's worst droughts? *Geophysical Research Letters*, 36(4).

Ushijima, Y., & Yoshikawa, Y. (2019). Mixed layer depth and sea surface warming under diurnally cycling surface heat flux in the heating season. *Journal of Physical Oceanography*, 49(7):1769-1787.

Wade, M., Caniaux, G., & du Penhoat, Y. (2011). Variability of the mixed layer heat budget in the eastern equatorial Atlantic during 2005-2007 as inferred using Argo floats. *Journal of Geophysical Research: Oceans*, 116(C8).

Wainwright, C. M., Finney, D. L., Kilavi, M., Black, E., & Marsham, J. H. (2020). Extreme rainfall in East Africa, October 2019-January 2020 and context under future climate change. *Royal Meteorological Society*, 76(1):26-31.

Waliser, D. E., Murtugudde, R., & Lucas, L. E. (2004). Indo-Pacific Ocean response to atmospheric

intraseasonal variability: 2. Boreal summer and the intraseasonal oscillation. *Journal of Geophysical Research: Oceans*, 109(C3).

Webster, P. J., Moore, A. M., Loschnigg, J. P., & Leben, R. R. (1999). Coupled oceanic-atmospheric dynamics in the Indian Ocean during 1997-98. *Nature*, 401:356-360.

Wisha, U. J., Dhiauddin, R., Rahmawan, G. A., & Wijaya, Y. J. (2021). Preliminary identification of causes to local coral bleaching event in Manjuto Beach, Pesisir Selatan Regency, West Sumatra: A hydro-oceanographic perspective. *Jurnal Ilmiah Perikanan dan Kelautan*, 13(2):156-170.

Wyrtki, K. (1961). Physical oceanography of the Southeast Asian waters. Cambridge: Cambridge University Press.

Xie, S. P., Du, Y., Huang, G., Zheng, X. T., Tokinaga, H., Hu, K., & Liu, Q. (2010). Decadal shift in El Niño influences on Indo-Western Pacific and East Asian climate in the 1970. *Journal of Climate*, 23:3352-3368.

Xue, T., Frenger, I., Prowe, A. E. F., José, Y. S., & Oschlies, A. (2021). Mixed layer depth dominates over upwelling in regulating the seasonality of ecosystem functioning in the Peruvian upwelling system. *European Geoscience Union*, 19(2):455-475.

Yoneyama, K., Zhang, C., & Long, C. N. (2013). Tracking pulses of the Madden-Julian oscillation. *Bulletin of the American Meteorological Society*, 94:1871-1891.

Yoshikawa, Y. (2015). Scaling surface mixing/mixed layer depth under stabilizing buoyancy flux. *Journal of Physical Oceanography*, 45(1):247-258.

Yu, J., Gan, B., Jing, Z., & Wu, L. (2020). Winter extreme mixed layer depth south of the Kuroshio extension. *Journal of Climate*, 33(24):10419-10436.

Yuan, D., Hu, X., Xu, P., Zhao, X., Masumoto, Y., & Han, W. (2018). The IOD-ENSO precursory teleconnection over the tropical Indo-Pacific Ocean: Dynamics and long-term trends under global warming. *Journal of Oceanology and Limnology*, 36:4-19.

Zhang, W., Wang, Y., Jin, F. F., Stuecker, M. F., & Turner, A. G. (2015). Impact of different El Niño types on the El Niño /IOD relationship. *Geophysical Research Letters*, 42(20):8570-8576.

Zhao, S., Jin, F. F., & Stuecker, M. F. (2019). Improved predictability of the Indian Ocean Dipole using seasonally modulated ENSO forcing forecasts. *Geophysical Research Letters*, 46:9980-9990.